

Structure of the Roper Resonance from Lattice QCD Constraints

Jia-jun Wu,¹ Derek B. Leinweber,¹ Zhan-wei Liu,^{1,2} and Anthony W. Thomas^{1,3}

¹*Special Research Centre for the Subatomic Structure of Matter (CSSM),
Department of Physics, University of Adelaide, Adelaide, South Australia 5005, Australia*

²*School of Physical Science and Technology,
Lanzhou University, Lanzhou 730000, China*

³*ARC Centre of Excellence for Particle Physics at the Terascale (CoEPP),
Department of Physics, University of Adelaide, Adelaide, South Australia 5005, Australia*

Two different descriptions of the existing pion-nucleon scattering data in the region of the Roper resonance are constructed. Both descriptions fit the experimental data very well. In one scenario the resonance is the result of strong rescattering between coupled meson-baryon channels, while in the other scenario, the resonance has a large bare-baryon (or quark-model like) component. The predictions of these two scenarios are compared with the latest lattice QCD simulation results in this channel. Consideration of the finite volume spectra, the manner in which the states are excited from the vacuum in lattice QCD and the composition of the states in Hamiltonian effective field theory enable a discrimination of these two different descriptions. We find the second scenario is not consistent with lattice QCD results whereas the first agrees with the lattice QCD constraints. In this scenario, the mass of the quark-model like state is approximately 2 GeV and in the finite volume of the lattice is dressed to place the first radial excitation of the nucleon at 1.9 GeV. Within this description, the infinite-volume Roper resonance is best described as a resonance generated dynamically through strongly coupled meson-baryon channels.

Since the discovery of the Roper resonance in 1964 [1], its peculiar properties have challenged our understanding of the quark structure of hadrons and ultimately of quantum chromodynamics (QCD) itself [2–20]. With the first negative-parity excitation of the nucleon, the $N^*(1535)$, almost 600 MeV higher in mass, expectations – based upon the harmonic oscillator model which has enjoyed much success in treating hadron spectroscopy – suggest that the first positive-parity excited state should occur at a little over 2 GeV. Yet, empirically one finds the first positive-parity, spin-1/2 Roper resonance of the nucleon to have a mass of just 1.45 GeV, *below* the $N^*(1535)$ [21]!

To make matters worse, the first negative parity excitation of a strangeness -1 baryon, the famous $\Lambda(1405)$, is lower in mass than both of these non-strange excited states of the nucleon [21]. Fortunately, in this case there have recently been advances in our understanding, thanks to modern lattice QCD simulations of not only the mass of this state but the individual valence quark contributions to its electromagnetic form factors [22, 23]. These simulations have also been supported by analysis involving an effective Hamiltonian [24], which allows a natural connection to be made between the results calculated on a finite lattice volume and the infinite volume of the real world [25, 26]. As a result of these studies, it is now clear that the $\Lambda(1405)$ is essentially an anti-kaon nucleon bound state with very little content corresponding to the sort of three-quark state anticipated in a typical quark model [23].

In this Letter, we use similar techniques to those which proved so successful for the $\Lambda(1405)$ [24] to investigate the nature of the Roper resonance. We first introduce the coupled channel scattering formalism [27] and show the two high quality fits obtained to existing data in the region of the Roper. In the first there is no significant three quark coupling, while in the second there is. These models produce rather different behaviour in the unobserved $\pi\Delta$ and σN channels and

cannot be distinguished by experiment. We then use the same models on a finite volume to compute the spectrum one would expect to find in lattice QCD. Only the first scenario is consistent with recent lattice simulations, indicating the Roper resonance is also generated dynamically through the rescattering of coupled meson-baryon channels. The three-quark state anticipated in traditional quark models appears to lie nearer 2 GeV, which as explained earlier, is far more consistent with the mass of the observed $N^*(1535)$.

In order to model the scattering data in the region of the Roper resonance and describe the observed inelasticity, we include three coupled channels, πN , $\pi\Delta$ and σN . In the rest frame, the Hamiltonian has the following form

$$H = H_0 + H_I, \quad (1)$$

where the non-interacting Hamiltonian is

$$H_0 = \sum_{B_0} |B_0\rangle m_B^0 \langle B_0| + \sum_{\alpha} \int d^3\vec{k} |\alpha(\vec{k})\rangle [\omega_{\alpha_1}(\vec{k}) + \omega_{\alpha_2}(\vec{k})] \langle \alpha(\vec{k})|. \quad (2)$$

Here B_0 denotes a bare baryon with mass m_B^0 , which may be thought of as a quark model state, α designates the channel and α_1 (α_2) indicates the meson (baryon) state which constitutes channel α . The energy $\omega_{\alpha_i}(\vec{k}) = \sqrt{m_{\alpha_i}^2 + \vec{k}^2}$.

The energy independent interaction Hamiltonian includes two parts, $H_I = g + v$, where g describes the vertex interaction between the bare particle and the two-particle channels α

$$g = \sum_{\alpha, B_0} \int d^3\vec{k} \{ |\alpha(\vec{k})\rangle G_{\alpha, B_0}^\dagger(k) \langle B_0| + h.c. \}, \quad (3)$$

while the direct two-to-two particle interaction is defined by

$$v = \sum_{\alpha, \beta} \int d^3\vec{k} d^3\vec{k}' |\alpha(\vec{k})\rangle V_{\alpha, \beta}^S(k, k') \langle \beta(\vec{k}')|. \quad (4)$$

For the vertex interaction between the bare baryon and the two-particle channels we choose:

$$G_{\alpha,B_0}^2(k) = \frac{g_{B_0\alpha}^2}{4\pi^2} \left(\frac{k}{f}\right)^{2l_\alpha} \frac{u_\alpha^2(k)}{\omega_{\alpha_1}(k)}, \quad (5)$$

where the pion decay constant $f = 92.4$ MeV and l_α is the orbital angular momentum in channel α . Here, since we are concerned with the Roper resonance, with isospin, angular momentum and parity, $\mathbf{I}(\mathbf{J}^P) = \frac{1}{2}(\frac{1}{2}^+)$, l is 1 for πN and $\pi\Delta$, while it is 0 for σN . The regulating form factor, $u_\alpha(k)$, takes the exponential form $u_\alpha(k) = \exp(-k^2/\Lambda_\alpha^2)$, where Λ_α is the regularization scale. For the direct two-to-two particle interaction, we introduce the separable potentials for the following five channels

$$V_{\alpha,\beta}^S(k, k') = g_{\alpha,\beta}^S \frac{\bar{G}_\alpha(k)}{\sqrt{\omega_{\alpha_1}(k)}} \frac{\bar{G}_\beta(k')}{\sqrt{\omega_{\beta_1}(k')}}, \quad (6)$$

where $\bar{G}_\alpha(k) = G_{\alpha,B_0}(k)/g_{B_0\alpha}$. The T -matrices for two particle scattering are obtained by solving a three-dimensional reduction of the coupled-channel Bethe-Salpeter equations for each partial wave

$$t_{\alpha,\beta}(k, k'; E) = V_{\alpha,\beta}(k, k'; E) + \sum_\gamma \int q^2 dq \times \quad (7)$$

$$V_{\alpha,\gamma}(k, q; E) \frac{1}{E - \omega_{\gamma_1}(q) - \omega_{\gamma_2}(q) + i\epsilon} t_{\gamma,\beta}(q, k'; E).$$

The coupled-channel potential is readily calculated from the interaction Hamiltonian

$$V_{\alpha,\beta}(k, k') = \sum_{B_0} \frac{G_{\alpha,B_0}^\dagger(k) G_{\beta,B_0}(k')}{E - m_{B_0}^0} + V_{\alpha,\beta}^S(k, k'), \quad (8)$$

with the normalization $\langle \alpha(\vec{k}) | \beta(\vec{k}') \rangle = \delta_{\alpha,\beta} \delta(\vec{k} - \vec{k}')$. The pole position of any bound state or resonance is obtained by searching for the poles of the T -matrix in the complex plane.

In order to compare the predictions of this continuum model with the results of lattice QCD simulations, it is necessary to rewrite the problem on a finite volume. This procedure is by now well known and we refer to Refs. [24, 25, 27–30] for the details. By solving for the eigenstates of the Hamiltonian effective-field-theory (EFT), one obtains energy levels which can be compared with the energies found in lattice QCD simulations. The eigenvectors of the Hamiltonian system describe the composition of the eigenstates which can be compared with the interpolating fields used to excite the lattice QCD states.

We can also extend the formalism to unphysical pion masses. Using m_π^2 as a measure of the light quark masses, we consider the variation of the bare mass and σ -meson mass as

$$m_B^0(m_\pi^2) = m_B^0|_{\text{phy}} + \alpha_B^0 (m_\pi^2 - m_\pi^2|_{\text{phy}}), \quad (9)$$

$$m_\sigma^2(m_\pi^2) = m_\sigma^2|_{\text{phy}} + \alpha_\sigma^0 (m_\pi^2 - m_\pi^2|_{\text{phy}}), \quad (10)$$

where the slope parameter α_B^0 is constrained by lattice QCD data from the CSSM. In the large quark mass regime, where

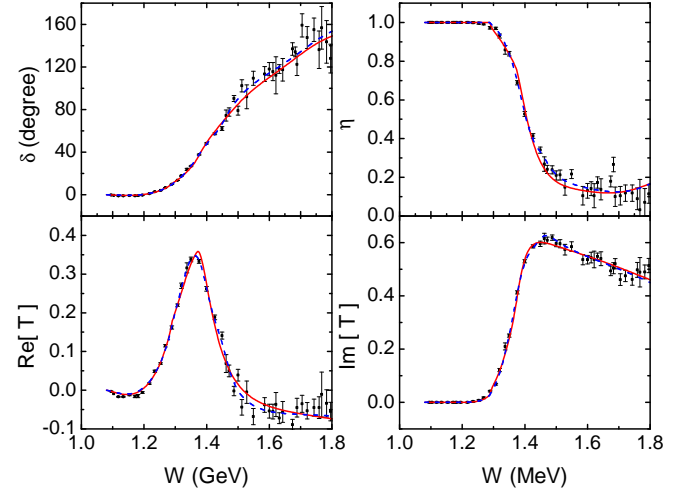


FIG. 1. The fitted phase shift δ , inelasticity η and T -matrix for the $\pi N \rightarrow \pi N$ reaction. Red-solid and blue-dashed lines are calculated from scenarios I and II, respectively.

constituent quark degrees of freedom become relevant, one expects [31] $\alpha_\sigma^0 = (2/3)\alpha_N^0$. The nucleon and Delta masses away from the physical point are obtained via linear interpolation between the lattice QCD results.

By fitting the experimental data for πN scattering from 1200 MeV to 1800 MeV, we found two rather different models which appear equally acceptable in terms of the quality of the fit to existing data. The corresponding parameters are shown in Table I. In Fig. 1, the phase shift, inelasticity and T -matrix for the $\pi N \rightarrow \pi N$ channel are shown for these two models. It is impossible to distinguish the merit of these two fits using the existing πN data. However, in the as yet unmeasured coupled channels there are considerable differences.

The main differences are that the coupling of $\pi N \rightarrow \pi N$ in fit I is much larger than that in fit II, while the coupling of the bare state to πN and σN in fit I is much smaller than in fit II. This leads to two different pictures of the Roper. In fit I it is a resonance generated by strong rescattering in the meson-baryon channels. On the other hand, in fit II the rescattering is weaker and the observed resonance is dominated by coupling to an underlying bare, or quark-model like, state.

In light of the present experimental data, these two scenarios are both acceptable. However, as illustrated in Fig. 2, measurements of the scattering amplitudes in the coupled channels $\pi\Delta \rightarrow \pi\Delta$ and $\sigma N \rightarrow \sigma N$, would enable us to distinguish between them.

Given the absence of the relevant experimental data, we now turn to the results provided by lattice QCD simulations, focussing on the recent work of Lang *et al.* [34] and the CSSM [27]. The former is particularly interesting as incorporated πN and σN five-quark non-local interpolating fields with the momenta of each hadron projected to provide excellent overlap with the low-lying scattering states of the spec-

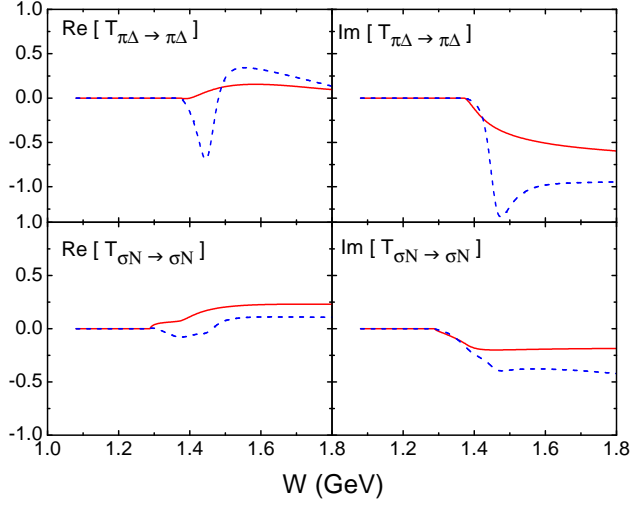


FIG. 2. The T -matrices for $\pi\Delta \rightarrow \pi\Delta$ and $\sigma N \rightarrow \sigma N$ corresponding to the two scenarios described in the text. The two cases are encoded as in Fig. 1.

trum. These are in addition to standard three-quark interpolating fields which have proved to favour localized states and miss the non-local scattering states [35–40] making the lattice spectrum incomplete. In reporting these results in Figs. 3 and 4 we have used solid(open) symbols to indicate states dominated by local(nonlocal) interpolating fields. This information can be used in addition to the standard analysis of the spectrum.

Just as insight into the composition of the lattice QCD states

TABLE I. Fit parameters constrained by πN scattering data and the resultant pole positions in the two scenarios described in the text. The pole position in the different Riemann sheets is also indicated. The unphysical sheet is denoted "u" and the physical sheet is denoted "p", as defined in Ref. [32, 33], and the order for the channels is $(\pi N, \pi\Delta, \sigma N)$.

Parameter	I	II
$g_{\pi N, \pi N}^S$	1.156	0.634
$g_{\pi N, \pi\Delta}^S$	-0.662	-0.378
$g_{\pi N, \sigma N}^S$	-0.415	-1.738
$g_{\pi\Delta, \pi\Delta}^S$	-0.438	-0.581
$g_{\pi\Delta, \sigma N}^S$	1.332	0.964
$g_{\sigma N, \sigma N}^S$	10.000	10.000
m_B^0/GeV	2.000	1.7000
$g_{B_0 \pi N}$	0.268	0.954
$g_{B_0 \pi\Delta}$	1.544	-0.118
$g_{B_0 \sigma N}$	—	-2.892
$\Lambda_{\pi N}/\text{GeV}$	0.5953	0.6302
$\Lambda_{\pi\Delta}/\text{GeV}$	1.5000	1.4318
$\Lambda_{\sigma N}/\text{GeV}$	1.5000	1.4533
Pole (MeV) (uuu)	2012.28 - 42.09 i	1355.57 - 70.81 i
Pole (MeV) (upu)	1392.92 - 167.13 i	1362.33 - 100.53 i

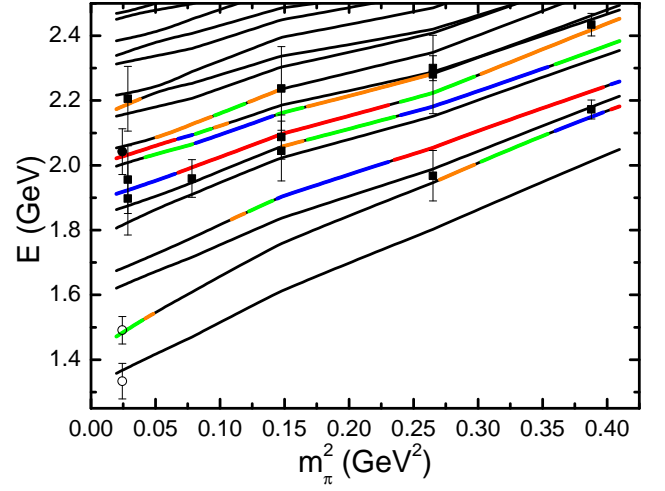


FIG. 3. The finite volume spectrum of Scenario I with a bare mass of 2.0 GeV. The CSSM results [27] are indicated by square symbols and circles denote the more recent results from Lang *et al.* [34]. Solid symbols indicate states dominated by local three-quark operators and open symbols indicate states dominated by non-local momentum-projected five-quark operators. The colours red, blue, green and orange are used to indicate the relative contributions of the bare baryon basis state in the eigenstate, with red being the largest contribution.

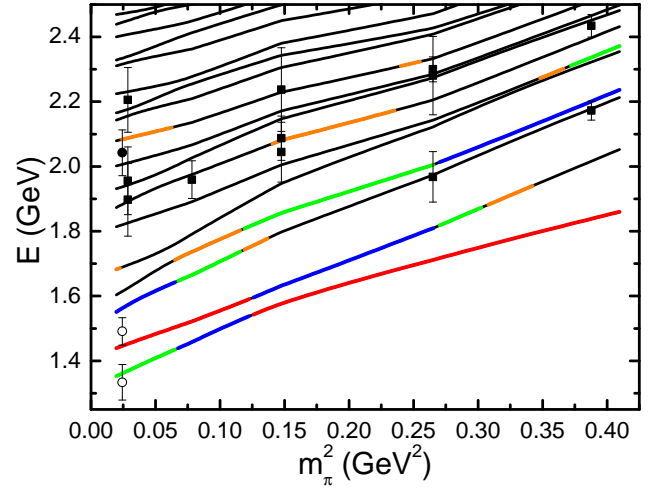


FIG. 4. The finite volume spectrum corresponding to Scenario II having a bare mass of 1.7 GeV. Results are illustrated as described in Fig. 3.

can be obtained from the eigenvectors of the lattice correlation matrix used to excite the states, Hamiltonian EFT also provides insight into their composition via the superposition of basis states for each eigenvector. In Figs. 3 and 4 we not only show the spectra calculated for Scenarios I and II but we also colour code the lines to indicate the amount of the bare-baryon (or three-quark) basis state in that particular eigenstate. The

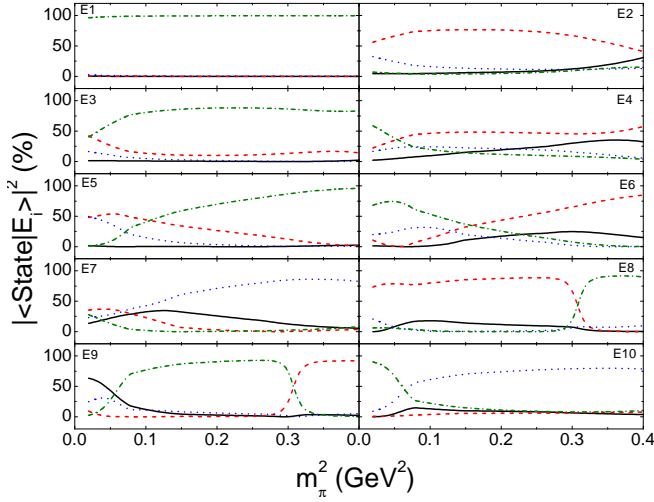


FIG. 5. The pion-mass evolution of the Hamiltonian eigenvector components for Scenario I having bare mass of 2.0 GeV. The black solid line indicates the fraction of the bare-state, $|\langle m_0 | E_i \rangle|^2$. The red dashed, blue dotted and green dashed-dotted lines show the πN , $\pi \Delta$ and σN contributions, summed over all discrete momenta, $\sum_{\vec{k}} |\langle \alpha(\vec{k}) | E_i \rangle|^2$. ("Ei" indicates the i'th energy level.)

red, blue, green and orange lines indicate the states having the first, second, third and fourth largest bare-state contributions, respectively.

For Scenario I, all of the lattice states dominated by local three-quark interpolating fields can be associated with a colored line. Similarly, all of the Hamiltonian states having the largest bare basis-state component, indicated in red in Fig. 3, have a nearby lattice QCD result. Thus, the predictions of Scenario I are consistent with lattice QCD.

On the other hand, Scenario II displays little correspondence to the lattice QCD results. Scenario II predicts a low-lying state with a large bare basis-state component of approximately 50%, approaching that for the ground state. Such a state would be easy to excite in lattice QCD with local three-quark operators. However this state is not seen in the simulations. The lattice state that is seen at light quark masses is actually excited by a πN scattering-state interpolating field. Indeed, Lang *et al.* [34] only see this state when they include a non-local πN interpolating field.

In Scenario I, the lattice excitation at $\simeq 1.5$ GeV is described by a Hamiltonian eigenstate dominated by the πN basis state. Fig. 5 shows the composition of the lowest ten Hamiltonian eigenstates as a function of pion mass for Scenario I. Near the physical mass the first eigenstate is dominated by σN basis states. Again, this is consistent with the work of Lang *et al.*, who only find the lowest state when they include a non-local σN interpolating field. The second state is dominated by the πN channel but some mixing with $\pi \Delta$ is also apparent. The $\pi \Delta$ channel dominates the fifth excitation of the spectrum at light quark masses and this serves as a

prediction for future lattice QCD calculations employing non-local momentum-projected $\pi \Delta$ scattering-state interpolators.

It is only for the seventh, eighth and ninth eigenstates that we find a significant bare basis-state contribution and this is precisely where the lattice QCD states excited by local three-quark operators reside. The ninth state has an extremely large bare-state component exceeding 50% and both the CSSM and Lang *et al.* observe lattice QCD eigenstates within one sigma of this state.

Next, we examine how the eigenstates evolve as the pion mass increases. Here one anticipates rescattering to become suppressed as the masses of the hadrons increase. In Fig. 5 we see that in scenario I the bare baryon content of the second and fourth eigenstates increases towards the upper end of the pion-mass range. Once again this is consistent with the lattice simulations as this is where the CSSM finds lower mass states in the spectrum with local three-quark operators. Overall the Hamiltonian eigenvectors obtained within Scenario I explain the lattice spectra very well.

In contrast, the content of the Hamilton eigenvectors in Scenario II is quite wrong. In particular, the lowest mass states are always dominated by the bare-baryon basis state and as noted before, this is inconsistent with the results of Lang *et al.*. Neither the CSSM nor the Cyprus collaboration [41] were able to identify such states in their lattice results.

In conclusion, the bare-baryon (or three-quark) basis state associated with the Roper resonance found in Nature lies at approximately 2 GeV. This large mass is required in order to provide a finite-volume spectrum consistent with lattice QCD. The result is also consistent with natural expectations from a harmonic oscillator spectrum. A lower bare basis-state mass leads to the prediction of quark-model like low-lying states dominated by a bare-state component. The absence of such states in the lattice QCD spectrum rules out this scenario.

In the preferred Scenario I with a 2 GeV bare-state mass, quark-model like states sit high in the spectrum. In the finite volume of the lattice, the bare state is dressed to produce states commencing at $\simeq 1.9$ GeV for the lightest pion mass of 156 MeV. Indeed, the CSSM studied the three-quark wave function of this state and discovered it resembles the first radial excitation of the quark model [42, 43].

With this new insight, the mystery of the low-lying Roper resonance may be nearing resolution. Evidence indicates the observed nucleon resonance at 1440 MeV is best described as the result of strong rescattering between coupled meson-baryon channels.

In working towards a definitive analysis there is ample scope for new data to further resolve the nature of this state. Better and more comprehensive experimental data on the channels coupled to the Roper resonance would be of significant interest. Further development of three-body channel contributions [44, 45] in effective field theory is desired. Similarly, a more comprehensive lattice QCD analysis of the *complete* nucleon spectrum in several lattice volumes would serve well to further expose the role of the coupled channels giving rise to the Roper resonance.

Acknowledgements: We thank the PACS-CS Collaboration for making their $2 + 1$ flavor configurations available and the ongoing support of the ILDG. This research was undertaken with the assistance of the University of Adelaide’s Phoenix cluster and resources at the NCI National Facility in Canberra, Australia. NCI resources were provided through the National Computational Merit Allocation Scheme, supported by the Australian Government and the University of Adelaide Partner Share. This research is supported by the Australian Research Council through the ARC Centre of Excellence for Particle Physics at the Terascale (CE110001104) and through Grants No. DP151103101 (A.W.T.), DP150103164, DP120104627 and LE120100181 (D.B.L.).

-
- [1] L. D. Roper, Phys. Rev. Lett. **12**, 340 (1964).
 - [2] I. G. Aznauryan *et al.* (CLAS), Phys. Rev. **C78**, 045209 (2008), arXiv:0804.0447 [nucl-ex].
 - [3] K. Joo *et al.* (CLAS), Phys. Rev. **C72**, 058202 (2005), arXiv:nucl-ex/0504027 [nucl-ex].
 - [4] H. J. Weber, Phys. Rev. **C41**, 2783 (1990).
 - [5] B. Julia-Diaz and D. O. Riska, Nucl. Phys. **A780**, 175 (2006), arXiv:nucl-th/0609064 [nucl-th].
 - [6] D. Barquilla-Cano, A. J. Buchmann, and E. Hernandez, Phys. Rev. **C75**, 065203 (2007), [Erratum: Phys. Rev. **C77**, 019903(2008)], arXiv:0705.3297 [nucl-th].
 - [7] B. Golli and S. Sirca, Eur. Phys. J. **A38**, 271 (2008), arXiv:0708.3759 [hep-ph].
 - [8] B. Golli, S. Sirca, and M. Fiolhais, Eur. Phys. J. **A42**, 185 (2009), arXiv:0906.2066 [nucl-th].
 - [9] U. G. Meissner and J. W. Durso, Nucl. Phys. **A430**, 670 (1984).
 - [10] C. Hajduk and B. Schwesinger, Phys. Lett. **B140**, 172 (1984).
 - [11] O. Krehl, C. Hanhart, S. Krewald, and J. Speth, Phys. Rev. **C62**, 025207 (2000), arXiv:nucl-th/9911080 [nucl-th].
 - [12] C. Schutz, J. Haidenbauer, J. Speth, and J. W. Durso, Phys. Rev. **C57**, 1464 (1998).
 - [13] A. Matsuyama, T. Sato, and T. S. H. Lee, Phys. Rept. **439**, 193 (2007), arXiv:nucl-th/0608051 [nucl-th].
 - [14] H. Kamano, S. X. Nakamura, T. S. H. Lee, and T. Sato, Phys. Rev. **C81**, 065207 (2010), arXiv:1001.5083 [nucl-th].
 - [15] H. Kamano, S. X. Nakamura, T. S. H. Lee, and T. Sato, Phys. Rev. **C88**, 035209 (2013), arXiv:1305.4351 [nucl-th].
 - [16] N. Suzuki, B. Julia-Diaz, H. Kamano, T. S. H. Lee, A. Matsuyama, and T. Sato, Phys. Rev. Lett. **104**, 042302 (2010), arXiv:0909.1356 [nucl-th].
 - [17] E. Hernandez, E. Oset, and M. J. Vicente Vacas, Phys. Rev. **C66**, 065201 (2002), arXiv:nucl-th/0209009 [nucl-th].
 - [18] T. Barnes and F. E. Close, Phys. Lett. **B123**, 89 (1983).
 - [19] E. Golowich, E. Haqq, and G. Karl, Phys. Rev. **D28**, 160 (1983), [Erratum: Phys. Rev. **D33**, 859(1986)].
 - [20] L. S. Kisslinger and Z. P. Li, Phys. Rev. **D51**, R5986 (1995).
 - [21] C. Patrignani *et al.* (Particle Data Group), Chin. Phys. **C40**, 100001 (2016).
 - [22] J. M. M. Hall, W. Kamleh, D. B. Leinweber, B. J. Menadue, B. J. Owen, A. W. Thomas, and R. D. Young, Phys. Rev. Lett. **114**, 132002 (2015), arXiv:1411.3402 [hep-lat].
 - [23] J. M. M. Hall, W. Kamleh, D. B. Leinweber, B. J. Menadue, B. J. Owen, and A. W. Thomas, (2016), arXiv:1612.07477 [hep-lat].
 - [24] Z.-W. Liu, W. Kamleh, D. B. Leinweber, F. M. Stokes, A. W. Thomas, and J.-J. Wu, Phys. Rev. Lett. **116**, 082004 (2016), arXiv:1512.00140 [hep-lat].
 - [25] Z.-W. Liu, J. M. M. Hall, D. B. Leinweber, A. W. Thomas, and J.-J. Wu, Phys. Rev. **D95**, 014506 (2017), arXiv:1607.05856 [nucl-th].
 - [26] R. Molina and M. Döring, Phys. Rev. **D94**, 056010 (2016), [Addendum: Phys. Rev. **D94**, no. 7, 079901(2016)], arXiv:1512.05831 [hep-lat].
 - [27] Z.-W. Liu, W. Kamleh, D. B. Leinweber, F. M. Stokes, A. W. Thomas, and J.-J. Wu, (2016), arXiv:1607.04536 [nucl-th].
 - [28] J. M. M. Hall, A. C. P. Hsu, D. B. Leinweber, A. W. Thomas, and R. D. Young, Phys. Rev. **D87**, 094510 (2013), arXiv:1303.4157 [hep-lat].
 - [29] J.-J. Wu, T. S. H. Lee, A. W. Thomas, and R. D. Young, Phys. Rev. **C90**, 055206 (2014), arXiv:1402.4868 [hep-lat].
 - [30] J.-J. Wu, H. Kamano, T. S. H. Lee, D. B. Leinweber, and A. W. Thomas, (2016), arXiv:1611.05970 [hep-lat].
 - [31] I. C. Cloet, D. B. Leinweber, and A. W. Thomas, Phys. Rev. **C65**, 062201 (2002), arXiv:hep-ph/0203023 [hep-ph].
 - [32] N. Suzuki, T. Sato, and T. S. H. Lee, Phys. Rev. **C79**, 025205 (2009), arXiv:0806.2043 [nucl-th].
 - [33] M. Doring, C. Hanhart, F. Huang, S. Krewald, and U. G. Meissner, Nucl. Phys. **A829**, 170 (2009), arXiv:0903.4337 [nucl-th].
 - [34] C. B. Lang, L. Leskovec, M. Padmanath, and S. Prelovsek, Phys. Rev. **D95**, 014510 (2017), arXiv:1610.01422 [hep-lat].
 - [35] M. S. Mahbub, W. Kamleh, D. B. Leinweber, P. J. Moran, and A. G. Williams (CSSM Lattice), Phys. Lett. **B707**, 389 (2012), arXiv:1011.5724 [hep-lat].
 - [36] M. S. Mahbub, W. Kamleh, D. B. Leinweber, P. J. Moran, and A. G. Williams, Phys. Rev. **D87**, 011501 (2013), arXiv:1209.0240 [hep-lat].
 - [37] M. S. Mahbub, W. Kamleh, D. B. Leinweber, P. J. Moran, and A. G. Williams, Phys. Rev. **D87**, 094506 (2013), arXiv:1302.2987 [hep-lat].
 - [38] M. S. Mahbub, W. Kamleh, D. B. Leinweber, and A. G. Williams, Annals Phys. **342**, 270 (2014), arXiv:1310.6803 [hep-lat].
 - [39] A. L. Kiratidis, W. Kamleh, D. B. Leinweber, and B. J. Owen, Phys. Rev. **D91**, 094509 (2015), arXiv:1501.07667 [hep-lat].
 - [40] A. L. Kiratidis, W. Kamleh, D. B. Leinweber, Z.-W. Liu, F. M. Stokes, and A. W. Thomas, (2016), arXiv:1608.03051 [hep-lat].
 - [41] C. Alexandrou, T. Leontiou, C. N. Papanicolas, and E. Stiliaris, Phys. Rev. **D91**, 014506 (2015), arXiv:1411.6765 [hep-lat].
 - [42] D. S. Roberts, W. Kamleh, and D. B. Leinweber, Phys. Lett. **B725**, 164 (2013), arXiv:1304.0325 [hep-lat].
 - [43] D. S. Roberts, W. Kamleh, and D. B. Leinweber, Phys. Rev. **D89**, 074501 (2014), arXiv:1311.6626 [hep-lat].
 - [44] M. T. Hansen and S. R. Sharpe, Phys. Rev. **D90**, 116003 (2014), arXiv:1408.5933 [hep-lat].
 - [45] M. T. Hansen and S. R. Sharpe, Phys. Rev. **D92**, 114509 (2015), arXiv:1504.04248 [hep-lat].